Kinetics Analysis of Electrophoretic Deposition Using Small and Large Signal Modeling: The Case Study of Nano-Mullite Suspension

Mohammad Sadegh Shakeri [1,*], Masood Alizadeh [2], Asghar Kazemzadeh [3], Touraj Ebadzadeh [4], Hossein Aghajani [5]

[1] Materials and Energy Research Center (MERC), P.O. Box 31779-83634, Karaj, Iran
[2] Department of Materials Engineering, University of Tabriz, Tabriz, Iran

ARTICLE INFO

ABSTRACT

Having sufficient and accurate understanding about kinetics of phenomena could be an important reason for further technological progresses. Finding a white-box mathematical model for weight vs. time curves of Electrophoretic Deposition (EPD) using large and small signal analysis has been thoroughly studied in the present investigation. Weight-Time curves of nano-Mullite suspension have been trained using the Simulink modeling tool. Results of the investigation illustrate that, the frequency of particles, i.e., the probability of particles collision with each other decreases due to the reduction of the particles concentration in the suspension. When the solid load becomes higher close to the electrode surface, the mobility of an individual particle will be restricted and a collective pressure onto the particles closer to the electrode surface is supposed to develop. The accumulated particles will be forced to flocculate and form a solid packing structure. According to the results of modeling, the times before flocculation are suitable for deposition of a highly dense coating.

1. Introduction
1.1. EPD and kinetics of deposition

Electrophoretic Deposition (EPD) is used as a practical method which is nowadays used for the coating of ceramic films in various fields of application such as biomaterials [1], electronic applications [2], thermal barrier coatings [3], and solar cells [4]. Simplicity of the coating procedure, low cost of equipment, ability to produce a uniform 3D coating and also simple control of thickness are the main characteristics of EPD technique which are the reasons for intensive attention of scientists and industries to this field of study [5]. EPD uses an electric field to accelerate the ionized particles in the stable suspension toward the opposing electrode and to depose a coating on it [6]. Under this condition, the particles move toward the electrode to form a dense film. Generally, EPD process is composed of two different steps; transition of charged particles in the solvent (Electrophoresis) and movement of them to form a solid layer on the electrode (Deposition) [7-10].

Mathematical modeling of EPD has been reported in some literatures. Gonzales-Cuenca et al. [13] reported the influence of deposit formation on deposit growth which is a refinement of the model described earlier by Biesheuvel and Verweij [14]. These models

---
* Corresponding author:
  E-mail: : ms.shakeri88@merc.ac.ir, Tel.: +98 9368980878, Fax: +98 2636280040-7

were extracted according to some ideal assumptions. Zhang et al. reported that the kinetic equation for deposited weight is an exponential equation [15]. Furthermore, Cordelair and Greil [16] used discrete element method (DEM) to gain insight into the kinetic of EPD [11-16].

1.2. Large and small signal analysis

Large-signal analysis is DC Analysis because the operating point and bias conditions of the circuit are found, which do not normally vary. It is done using the current and voltage equations that describe the active device. Once the large signal values are found, the "small-signal" parameters can be established [17-19]. Small-signal analysis is AC Analysis because the signals vary around the DC bias condition, i.e. a small AC source slightly increases and decreases the bias point to produce a signal. In small-signal analysis, the device will be linearized by replacing the non-linear device with linear ones such as voltage dependent resistors and sources. It works because the instantaneous slopes of the I-V curve at values very close to a particular DC point look quite linear. In general, small-signal model uses values for the parameters that are found in large-signal Analysis [20-25].

In the present investigation, an attempt has been made to thoroughly investigate the kinetics of deposition process in EPD using small and large signal analyses. Although there are numerous investigations related to the kinetics of the EPD process, the present one will discuss the issue in more details. In this regard, large signal analysis is done using Equivalent Circuit Modeling (ECM) and accordingly small signal analysis will utilize the Simulink modeling toolbox. The motivation of this investigation is to use the resulting model in industrial applications for prediction of the EPD process.

2. Materials and methods
2.1. Nano-Mullite synthesis using the sol-gel method

For synthesis of nano-Mullite with stoichiometric composition of $3Al_2O_3.2SiO_2$, the following procedure was done. Initially, $Al(NO_3)_3.9H_2O$ was dissolved in distilled water. The solution was heated up to 60 °C for 1 h on a magnetic stirrer. Dissolved $(C_2H_5O)_4Si$ in ethanol was added to the nitrate solution dropwise. For making the gel, the resulted solution was heated up to 60 °C for 4 h on the magnetic stirrer. The resulted gel was dried in air for 3 days and calcination heat treatment was done at 1400 °C for 2 h. Unisantis XMD 300 X-ray diffractometer was used for determination of the phases and the crystalline size of the powder. Furthermore, in order to calculate Zeta potential and particle size distribution, Dynamic Light Scattering (DLS, Nanotrac Wave, USA) was utilized.

2.2. Suspension preparation and the deposition process

The suspension was prepared by adding 4 gr of nano Mullite powder to 50 ml of Ethanol. Furthermore, 20 ml/l triethylamine (TEA) was added as the dispersant. The suspension was put on a magnetic stirrer (Alfa D-500, Iran) for 45 min and in an ultrasonic bath (Hielscher model UP 100 H, Ultrasound Technology, Germany) for 45 min in order to be suitably dispersed. To prevent the particles from settling, the suspensions were placed on a magnetic stirrer for 5 min before each deposition process. Conductivity and pH of the suspensions were found to be 9.1 μ c $^{-1}$ and 6.9, respectively (measurements were done by Metrohm, 827 pH lab, and Metrohm, 712 conduct meter).

Surface preparation of C-C composite samples was performed by grinding up to 800 grit using SiC papers followed by cleaning successively in acetone and ethanol using an ultrasonic bath for 45 min. Then the samples were washed with distilled water and dried in air.

An electrophoretic cell contained a 150 ml beaker, a C-C composite electrode as anode with surface area of 10×10 mm, and the same sample with as cathode and a fixer to fix the location of electrodes. The electrodes were set within 1 cm distance from each other. During electrophoretic deposition, constant voltages of 40, 60, and 80 V were applied by a power supply (Mastech, DC power supply HY30001E, 9225) and the changes of electric current during deposition were measured by means of Escort, 3146A Dual Display Multi meter. The samples were dried in desiccators for 24 h after the deposition process to be ready for weight measurements.

2.3. Modeling procedure

Modeling of electrophoretic deposition process was done using the Simulink modeling toolbox of MATLAB software. Large signal modeling was done using equivalent circuit modeling due to the correspondence of particle deposition curves with the charging of a reservoir in a simple RC circuit. Simultaneous AC and DC currents were set for the circuit. Physical assumptions were utilized. Accordingly, response of the circuit was presented and studied for each assumption. Last but not least, a complete model with all assumptions was represented.

3. Results and Discussion

3.1. Characterization of nano-Mullite powder

Fig. 1 shows the XRD pattern of the as-synthesized powder. As it is illustrated, there is a suitable correspondence between the peaks of the pattern with those for orthorhombic Mullite phase in the reference card No. 00-006-0259. It shows that if there are other phases such as remaining alumina, their amounts are so low that they could be neglected. No diffracted peaks other than those from Mullite are obtained in the pattern, indicating high purity of the as-synthesized products. Strong and sharp peaks

suggest that the as-synthesized product is well crystallized.

Using Scherer equation and Expert software, the size of powder crystals was calculated to be 32 nm. It is almost obvious that the size of the powder is more important than the size of crystals in the deposition part of the EPD process. Accordingly, the size of the powder was calculated using dynamic light scattering (DLS) method in stable suspension. DLS calculates the particle size, Zeta potential and molecular weight using Brownian movement of the particles in a liquid medium. Zeta potential of the suspension was determined to be 51.2 mV.

Fig. 2 shows the DLS results of nano-Mullite powder which demonstrate the distribution of particles in the electrolyte. As can be seen, the average size of particles is about 50 nm. The particles are distributed in the range of 36.4 to 59.8 nm. There is also the probability of existence of smaller and larger particles which is not reported in fig. 2 because those ranges are fewer than 10% of quantity.

Fig. 3 illustrates the DLS results for volume and surface distribution of the particles. As it is illustrated, the average surface area and volume of particles are approximately the same which could be a characterization of fine spherical
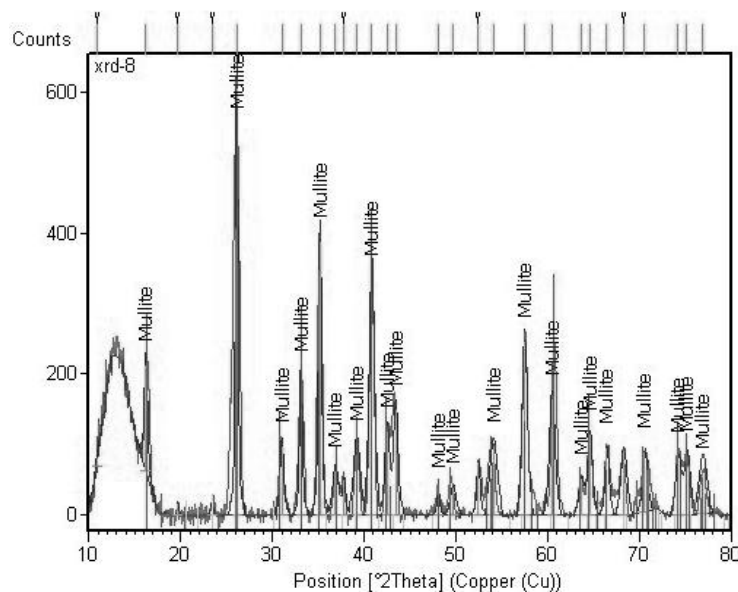

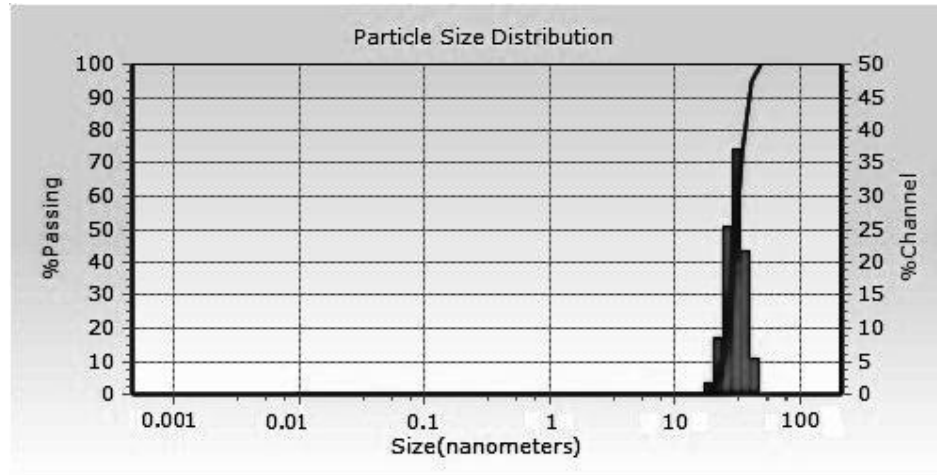
Fig. 1. XRD pattern of the as-synthesized nano-Mullite

Fig. 2. DLS curve showing the distribution of particles in the electrolyte for nano-Mullite powder
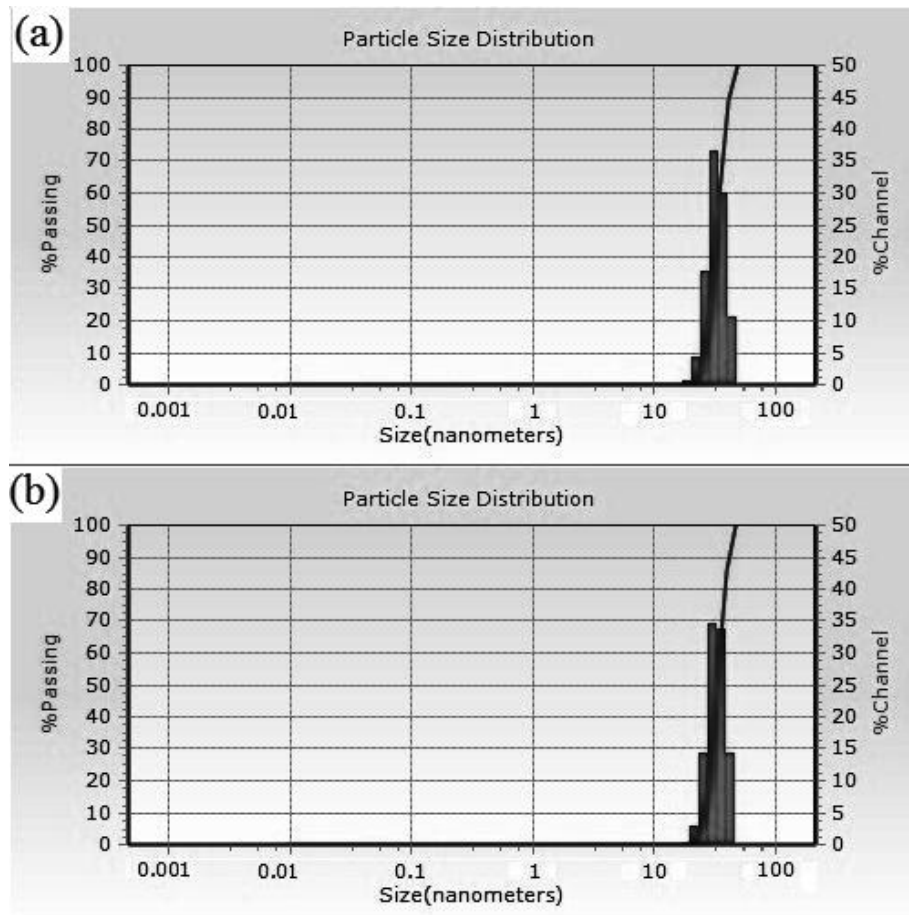

Fig. 3. DLS curve showing volume and surface distribution of particles for nano-Mullite powder

3.2. Large signal analysis

Fig. 4 depicts the coating weight vs. time curves for samples coated at 40, 60 and 80 V. As it is illustrated, gradient of curves decreases gradually
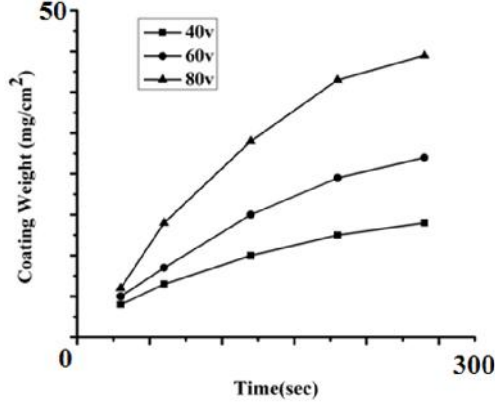

Fig. 4. Coated weight vs. time curves

With increasing of the applied voltage, the coating weight increases intensively. According to equivalent circuit modeling, there should be an electric circuit one of the components (V-t plot) of which is similar to fig. 4. Charging of a reservoir in an RC circuit has gotten the same plot. Accordingly, the corresponding equation for the curves in fig. 4 is as follow:

$$w = w_M(1 - e^{-k}) \tag{1}$$

Where w is the coated weight at time t, w_M is the amount of powder in the suspension and k is a kinetic constant that depends on the voltage of the electrophoretic deposition process, composition of suspension and so on. Kinetic constant will be discussed more in the following section. It is also noticeable that fitness of Eq. (1) could lead to a similar equation.

As mentioned, fig. 1 and Eq. (1) are the same as those for charging of a reservoir in RC circuit. Charging of a reservoir vs. time has been determined as

$$v = v_I(1 - e^{-\frac{1}{R}*t}) \tag{2}$$

There is a one to one correspondence between the parameters in Eq. (1) and (2). Consequently, k corresponds to 1/RC. R and C are defined by

$$R = {}^{\rho}/_A \tag{3}$$

and

$$C = {}^{\varepsilon_i}/_L \tag{4}$$

Where   is the specific resistivity, L is the distance between electrodes, A is the cross section of the anode, and   is the dielectric constant of the suspension.

If behavior of electrophoretic deposition is considered as a RC circuit, the electrophoretic cell could have twofold characterization of resistor and reservoir together. As a result, the constant value of k corresponding to 1/RC could be calculated as

$$k = 1/R = 1/\rho \tag{5}$$

Both   and   are the inherent parameters of suspension [26]. Furthermore,   and   will be varied in different temperatures and voltages. Hence, k constant depends on the composition and temperature of suspension as same as the voltage of electrophoretic deposition process.

The kinetic model which is introduced in Eq. (1) is the same as the model reported by Zhang et al. previously. There are two differences between these two models. Firstly, equivalent circuit modeling was a more routine method-- for extraction of model which is used in this article. Secondly, the introduced equation for kinetic constant (k) is very simple and easy to calculate in comparison with Zhang's kinetic constant.

Fig. 5 shows the large signal of model for each 3 deposited samples depicted by DC current in Simulink.
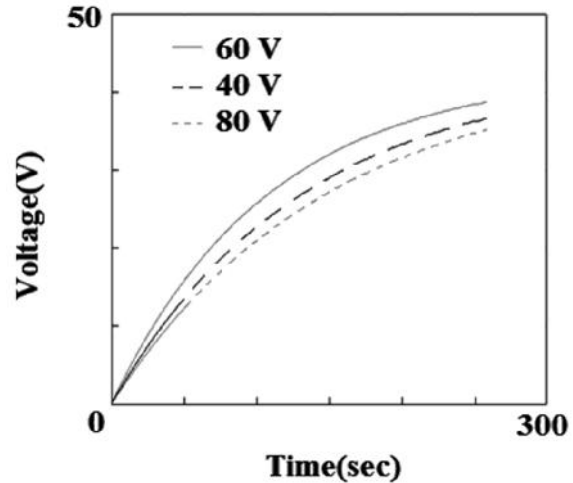

Fig. 5. The response of large signal modeling

There is a good correspondence between the curves of fig. 4 and fig. 5, with the R-square being more than 95%. This is an important factor

because this model is used for the following small signal modeling procedure.

3.3. Small signal analysis
3.3.1. Boundary conditions
For the calculation of small signal modeling, some information is needed that would be discussed below. Fig. 6 depicts V vs.   for the RC circuit.

As it is illustrated, by reduction of frequency, the voltage of reservoir will increase till it reaches to V_0 at   = 0.

By increasing the deposited weight, the concentration of powder in the suspension decreases, resulting in the reduction of activation energy. Assume that electrophoretic deposition starts at a specified frequency. Because of the high frequency, some of the suspended particles deposit on the electrode. The activation energy will decrease due to the reduction of powder concentration in the suspension. Therefore, the frequency of particles in the suspension will decrease. The frequency can be interpreted as the probability of suspended particles for collision to other particles. This process could continue to near zero frequencies.

The coated weight could change alternatively and so it can be represented by

$$w = w_M \sin \omega \tag{6}$$

Hence, it is predictable that large signal response of circuit (fig. 5) will be alternative around the fitted exponentially line. So, the input for the model could be defined discretely and step by step by

$$w_1 = w_{M1} \sin \omega_1 t \tag{7}$$
$$w_2 = w_{M2} \sin \omega_2 t \tag{8}$$
and
$$w_n = w_M \ \sin \omega_n t \tag{9}$$

Moreover, the boundary conditions for electrophoretic deposition modeling are as follows:

$$\begin{cases} t = 0 \ \to \ \Delta W = W_T \\ t = t_T \ \to \ \Delta W = 0 \end{cases} \tag{10}$$

and

$$\begin{cases} t = 0 \ \to \ \omega = \omega_T \\ t = t_T \ \to \ \omega = 0 \end{cases} \tag{11}$$

3.3.2. AC modeling with constant W and ω
In each frequency, a sinusoidal equation like Eq. (6) has been set as an input for AC modeling of electrophoretic deposition process (Fig. 7-A). Fig. 7-B shows the schematic of the output of the model.

As it is illustrated in Fig. 7-B, when frequency is constant, accumulation of the coated weight decreases exponentially. The coated weight in a constant   and W could be expressed by

$$w = w_M \left[\frac{s \ \omega + (e^{-t/k} - c \ \omega)\omega}{1 + \omega^2 k^2} \right] \tag{12}$$
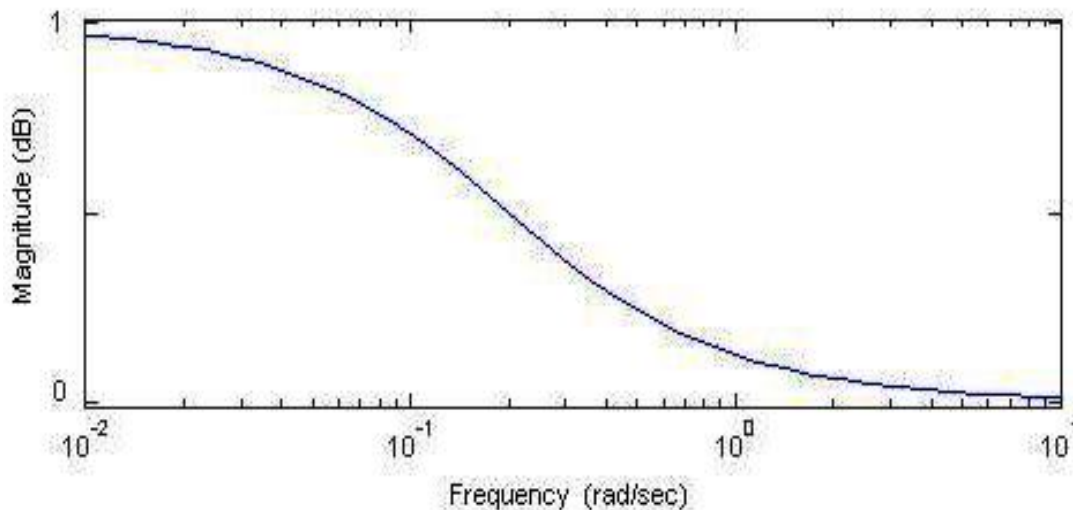

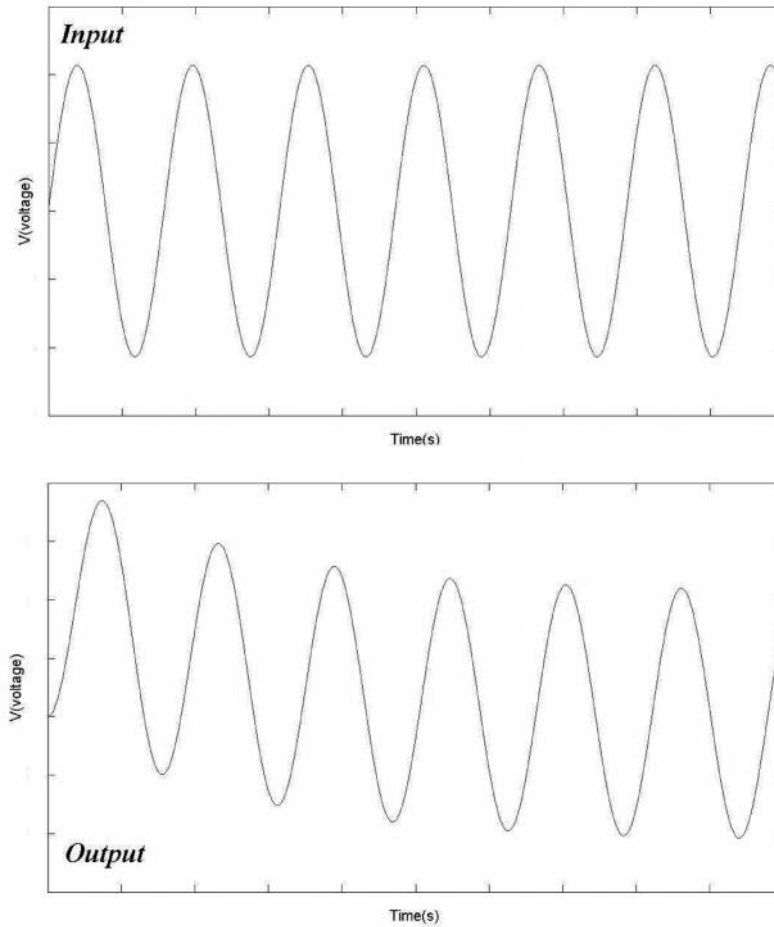**Fig. 6.** Variation of the magnitude of reservoir voltage in different frequencies [24]

Fig. 7. Input and output of the model (Eq. 2) running with an AC current

3.3.3. AC modeling with constant W and variable ω

According to Fig. 6, it can be mentioned that with a little approximation, frequency of particles decreases exponentially as

$$\omega = \omega_0 e^{-k} \qquad (13)$$

Fig. 8 illustrates input and output of the model when the frequency of particles changes.

In this case, the input of the model is defined by Eq. (6) and, as a result, the output of the model will be expressed by

$$w = w_M \int_0^t \sin(\omega_0 e^{-k} \tau) e^{\frac{-t+\tau}{k}} d \qquad (14)$$

3.3.4. AC modeling with variable W and constant ω

According to Eq. 1, the coated weight increases exponentially. Therefore, the weight of powder in the suspension changes as

$$W = W_T e^{-k} \qquad (15)$$

If the concentration of particles in the suspension decreases while the atoms frequency remains constant, Fig. 9 shows the input and output of the model.

In this case, the output of the model can be expressed by

$$W = \frac{W_T e^{-t/k(1-c\ (\omega\ ))}}{k} \qquad (16)$$

3.3.5. AC modeling with variable W and ω

In the EPD process, both frequency and powder concentration in suspension change simultaneously. Fig. 10 depicts the input and output of the model while frequency and powder
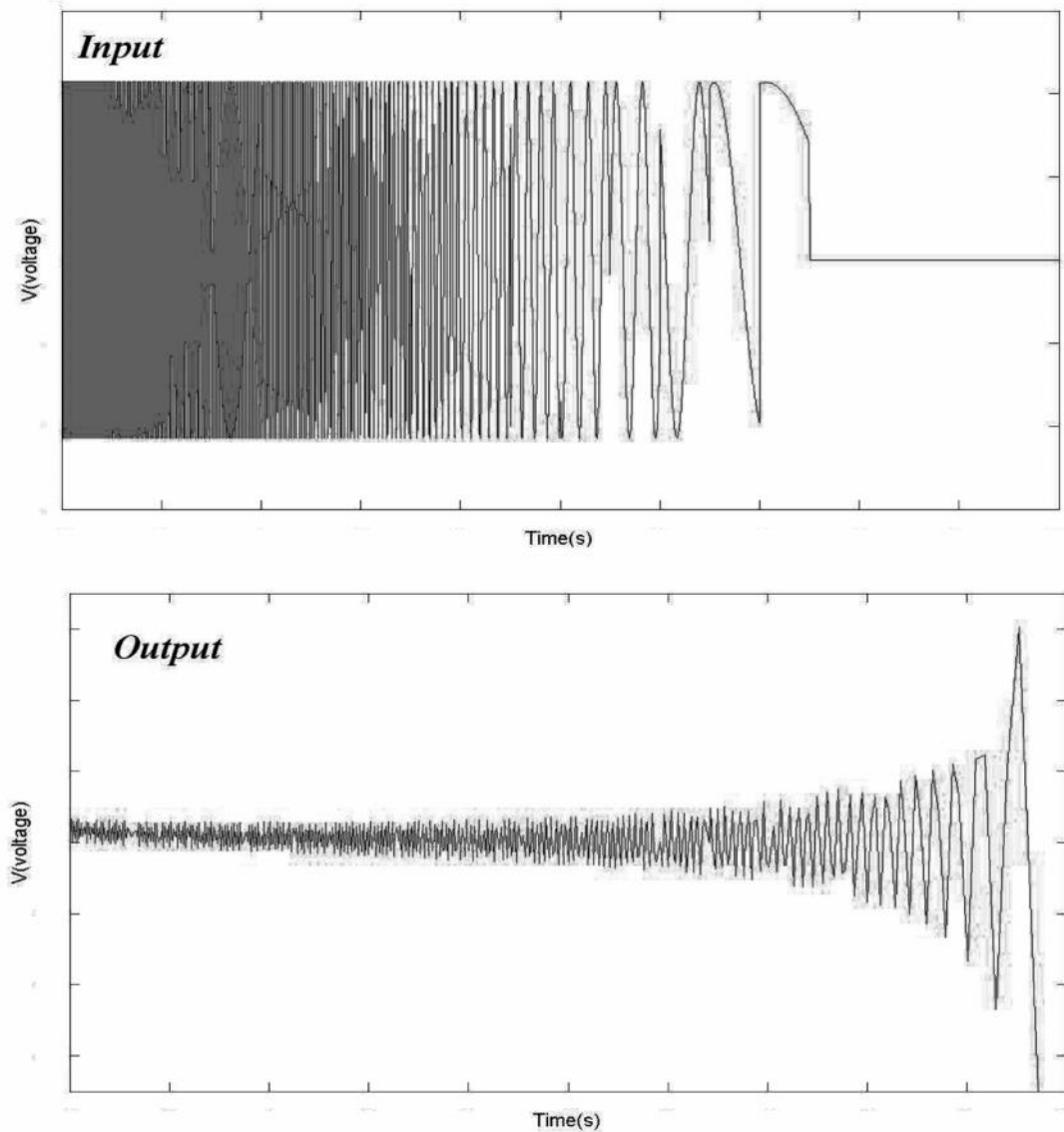
Fig. 8. Input and output of the model when the frequency of particles changes

concentration change simultaneously.
When the input of the model is defined by variable   Eq. (6) and W Eq. (15), then the output will be defined by

$$W = W_T \int_0^t \sin(\omega_0 e^{-k} \tau) e^{\frac{-t+\tau}{k}} d \qquad (17)$$

According to fig. 10-B, there is an intensive drop of voltage in the range of 2-3 minutes of the deposition process. This could be interpreted as the time for flocculation of particles. When the solid load becomes higher close to the electrode surface, the mobility of individual particle will be restricted and a collective pressure onto the particles closer to the electrode surface is supposed to develop. The accumulated particles will be forced to flocculate and form a solid packing structure. Flocculation causes a drop in the frequency of particles the same as the deposition of mass. Accordingly, the times before flocculation are suitable for having a uniform dense coating

3.4. Simultaneous small and large signal modeling

Large- and small-signal analysis was separately modeled for electrophoretic deposition process. The sum of these two models gives the complete model of deposition in the electrophoretic process that is defined by

$$W = W_I(1 - e^{-k} + \int_0^t \sin(\omega_U e^{-k} \tau)e^{\frac{-t+\tau}{k}}d \ ) \quad (18)$$

Fig. 11 depicts the output of the model for each three deposited samples gained from Eq. (18). As it is illustrated, there is a periodic variation (small signal) on all curves (large signal). It means that there is a noise on general changes of deposition. This noise was modeled using small signal analysis. The equations which are

expanded for EPD kinetics could give some useful information about the EPD process. A distinct feature of EPD or any other colloidal processing of ceramics is the large area of contact between the particles and the dispersing medium. Hence, surface forces strongly influence the suspension behavior and power packing density during deposition. Having knowledge about frequency of the collision of particles in suspension could be used as a priority for making a suitable dense coating. Eq. (14), (17), and (18) show the frequency changes. When the frequency is minimal, the high packed coating will be deposited.
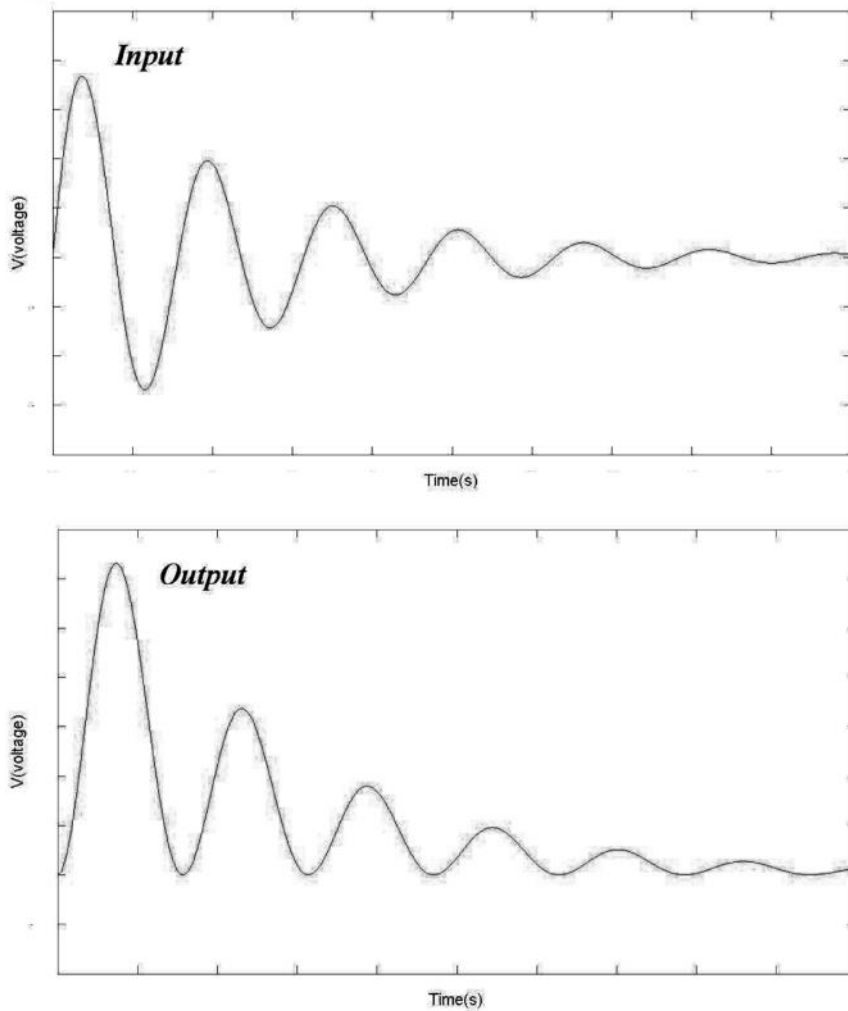

Fig. 9. Input and output of the model while the concentration of particles in the suspension decreases and the frequency of atoms remains constant
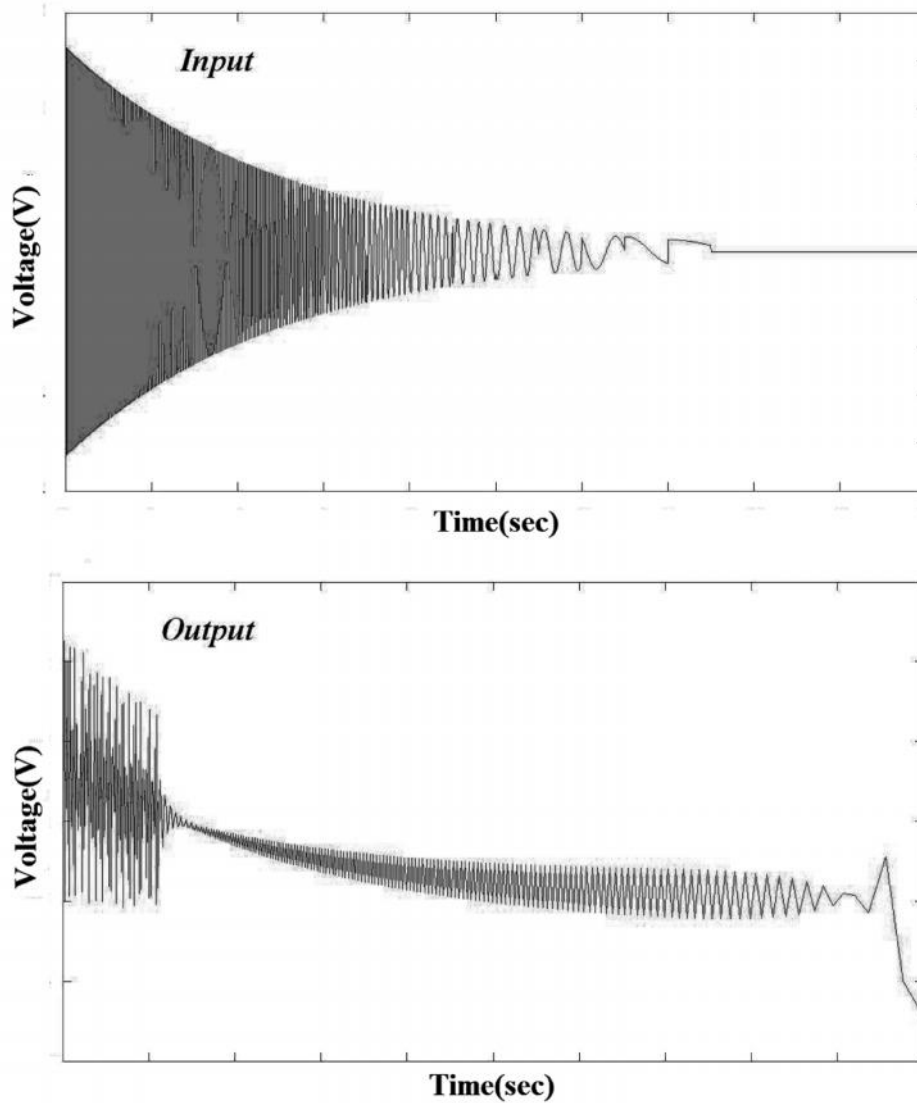
Fig. 10. The input and output of the model while frequency and powder concentration change simultaneously
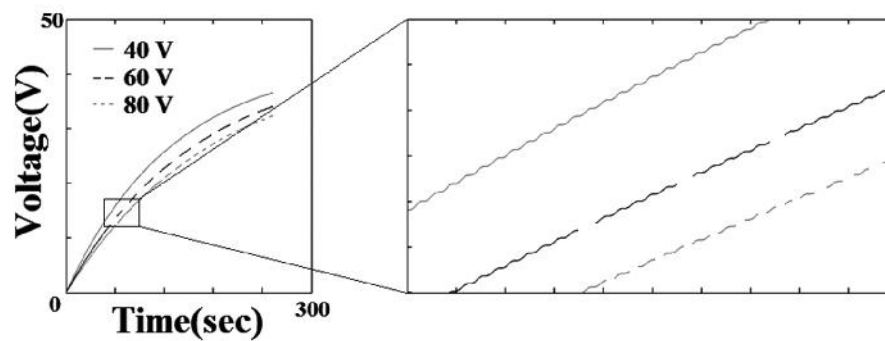

Fig. 11. Output of model for each three deposited samples gained from Eq. (18)

4. Conclusions

- According to equivalent circuit modeling (ECM), the coating process in electrophoretic deposition is completely comparable with charging of reservoir in an RC circuit.

- During the electrophoretic deposition process, the frequency of particles, i.e., the probability of particles collision with each other decreases due to the reduction of the concentration of particles in suspension.

- When the solid load becomes higher close to the electrode surface, the mobility of individual particle will be restricted and a collective pressure onto the particles closer to the electrode surface is supposed to develop. The accumulated particles will be forced to flocculate and form a solid packing structure which is a reason for a drop in coating quality. The resulted model correctly shows and predicts this drop.

References

[1] I. Corni, M.P. Ryan, A.R. Boccaccini, "Electrophoretic deposition: From traditional ceramics to nanotechnology", *J. Euro. Ceram. Soc*, Vol. 28, 2008, pp.1353–1367.

[2] J.C. Huang, Y.J. Ni, Z.C. Wang, "Preparation of hydroxyapatite functionally gradient coating on titanium substrate using a combination of electrophoretic deposition and reaction bonding process", *Surf. Coat. Tech*, Vol. 204, 2010, pp.3387–3392.

[3] J. Huang, W. Yang, L. Cao, "Preparation of a SiC/Cristobalite-AlPO4 Multi-layer Protective Coating on Carbon/Carbon Composites and Resultant Oxidation Kinetics and Mechanism", *J. Mater. Sci. Tech*, Vol. 26, 2010, pp.1021-1026.

[4] K. Hasegawa, S. Kunugi, M. Tatsumisago, T. Minami, "Preparation of thick films by electrophoretic deposition using modified silica particles derived by sol–gel method", J. Sol–gel. Sci. Tech, Vol. 15, 1999, pp.243–249.

[5] W. Shan, Y. Zhang, W. Yang, C. Ke, Z. Gao, Y. Ke, "Electrophoretic deposition of nano-size zeolites in non-aqueous medium and its application in fabricating thin zeolite membranes", Micropor. Mesopor. Mater., Vol. 69, 2004, pp.35–42.

[6] M. Wei, A.J. Ruys, B.K. Milthorpe, C.C. Sorrell, J.H. Evans, "Electrophoretic deposition of hydroxyapatite coatings on metal substrate: a nano-particulate dual coating approach", J. Sol–gel. Sci. Tech, Vol. 21, 2001, pp.39–48.

[7] T.M. Sridhar, U.K. Mudali, "Development of bioactive hydroxyapatite coatings on Type 316L stainless steel by electrophoretic deposition for orthopedic applications", Trans. Ind. Inst. Met, Vol. 56, 2003, pp. 221–230.

[8] J.H. Yum, S.Y. Seo, S. Lee, Y.E. Sung, "$Y_3Al_5O_{12}:Ce_{0.05}$ phosphor coating on gallium nitride for white light emitting diodes", J. Electrochem. Soc, Vol. 150, 2003, pp. 47–52.

[9] H.S. Maiti, S. Datta, R.N. Basu, "High Tc superconductor coating on metal substrates by an electrophoretic technique", J. Am. Ceram. Soc, Vol. 72, 1989, pp. 1733–1735.

[10] G. Wang, P. Sarkar, P.S. Nicholson, "Influence of acidity on the electrostatic stability of alumina suspensions in ethanol", J. Am. Ceram. Soc, Vol. 80, 1997, pp. 965–972.

[11] D.R. Brown, F.W. Salt, "The mechanism of electrophoretic deposition", J. Appl. Chem, Vol. 15, 1965, pp. 40–48.

[12] R.N. Basu, C.A. Randall, M.J. Mayo, "Fabrication of dense zirconia electrolyte films for tubular solid oxide fuel cells by electrophoretic deposition", J. Am. Ceram. Soc, Vol. 84, 2001, pp. 33–40.

[13] M. Gonzalez-Cuenca, P.M. Biesheuvel, H. Verweij, "Modeling constant voltage electrophoretic deposition from stirred suspension", J. AIChE, Vol. 46, 2000, pp. 626–631.

[14] P.M. Biesheuvel, H. Verweij, "Theory of cast formation in electrophoretic deposition", J. Am. Ceram. Soc, Vol. 82, 1999, pp. 1451–1455.

[15] Z. Zhang, Y. Huang, Z. Jiang, "Electrophoretic deposition forming of SiC-TZP composites in nonaqueous sol", J. Am. Ceram. Soc, Vol. 77, 1994, pp. 1946–1949.

[16] Y.C. Wang, I.C. Leu, M.H. Hon, "Kinetics of electrophoretic deposition for nanocrystalline zinc oxide coatings", J. Am Ceram. Soc, Vol. 87, 2004, pp. 84–88.

[17] C. Jacoboni, P. Lugli, The Monte Carlo Method for Semiconductor Device Simulation, First ed., Springer-Verlag, Berlin, 1989.

[18] S. Selberherr, Analysis and Simulation of Semiconductor Devices, Second ed., Springer-Verlag, Berlin, 1984.

[19] T. Grasser, Advanced Device Modeling and Simulation, First ed., World Scientific, London, 2003.

[20] K. Kramer, M. Kevin, W. Hitchon, G. Nicholas, Semiconductor devices: a simulation approach, 3rd ed., Prentice Hall, London, 1997.

[21] D. Vasileska, S. Goodnick, Computational Electronics, Second ed., Morgan & Claypool, New York, 2006.

[22] C. Galup-Montoro, M.C. Schneider, Mosfet Modeling for Circuit Analysis and Design, First ed., World Scientific, London, 2007.

[23] N. Arora, Mosfet Modeling for VLSI Simulation: Theory and Practice, First ed.,World Scientific, London, 2007.

[24] Y. Tsividis, Operational Modeling of the MOS Transistor, Second ed., McGraw-Hill, New York, 1999.

[25] K. Munshi, "Small Signal and Large Signal Modeling of HBT's Using Neural Networks", Microwave Review, Vol. 75, 2003, pp. 31-34.

[26] H.G. Davies, R.J. Rogers, "The Vibration of Structures Elastically Constrained at Discrete Points", J. Sound Vibration, 1979, pp. 437-447.